View metadata, citation and similar papers at core.ac.uk

brought to you by CORE

provided by University of Bath Research Portal

Citation for published version:
Mohammed, HA & Bending, SJ 2014, 'Fabrication of nanoscale Bi Hall sensors by lift-off techniques for applications in scanning probe microscopy', Semiconductor Science and Technology, vol. 29, no. 8. https://doi.org/10.1088/0268-1242/29/8/085007

DOI:
10.1088/0268-1242/29/8/085007

Publication date:
2014

Document Version
Peer reviewed version

Link to publication

University of Bath

General rights
Copyright and moral rights for the publications made accessible in the public portal are retained by the authors and/or other copyright owners and it is a condition of accessing publications that users recognise and abide by the legal requirements associated with these rights.

Take down policy
If you believe that this document breaches copyright please contact us providing details, and we will remove access to the work immediately and investigate your claim.

Download date: 13. May. 2019

Fabrication of nanoscale Bi Hall sensors by lift-off techniques for applications in scanning probe microscopy

H A Mohammed[1,2], and S J Bending[1]

[1]*Department of Physics, University of Bath, Bath BA2 7AY, UK*
[2]*Department of Physics, University of Kirkuk, Kirkuk, Iraq*
E-mail: hamm20@bath.ac.uk

Abstract

Bismuth Hall effect sensors with active sizes in the range 0.1 - 2 μm have been fabricated by electron beam lithography and lift-off techniques for applications in scanning Hall probe microscopy. The Hall coefficients, offset resistances and minimum detectable fields of the sensors have been systematically charecterised as a function of device size. The miniumum detectable field of 100 nm probes at 300K and dc currents of 5 μA is found to be B_{min}=0.9 mT/$Hz^{0.5}$ with scope for up to a factor of ten reductions by using higher Hall probe currents. This is significantly lower than in similar samples fabricated by focussed ion beam (FIB) milling of continuous Bi films, suggesting that the elimination of FIB damage and Ga^+ ion incorporation through the use of lift-off techniques leads to superior figures of merit. A number of ways in which the room temperature performance of our sensors could be improved still further are discussed.

Introduction

Magnetic Force Microscopy (MFM) [1, 2] is currently the accepted tool in the data storage industry for characterising the nanoscale magnetisation distribution in ferromagnetic media, particularly ferromagnetic domains and domain walls. Magnetic Force Microscopy is a scanning probe technique that measures the force between an oscillating magnetically-coated tip and the sample, and suffers from two characteristic weaknesses. Firstly, the sharp magnetic tip is invasive and can perturb the magnetic structure of the sample (or vice versa). Secondly, the micromagnetic structure of the tip is rarely known with any confidence, rendering imaging results qualitative rather than quantitative in most cases. Consequently there is a key outstanding requirement for a quantitative and non-invasive imaging technique to complement MFM. Moreover, this new technique must operate effectively at room temperature, since it is generally undesirable to cool ferromagnetic samples

cryogenically for characterisation. One promising candidate technique is scanning Hall probe microscopy (SHPM) [3]. This is a non-invasive scanning probe imaging technique whereby a nanoscale Hall effect sensor is used to map the local magnetic induction close to the surface of a magnetic sample, and provides quantitative data on at least one component of the magnetic induction vector. It has been widely used for investigating flux structures in superconductors at low temperatures, but has not been extensively used at room temperature, due to the typically poor minimum detectable fields at 300 K. As a consequence, recent developments in the field have focused on designing and fabricating novel nanoscale Hall sensors with lower noise figures at room temperature.

In order to achieve high spatial resolution SHPM sensors need to be fabricated with nanoscale dimensions and operated in very close proximity to the sample surface. High magnetic field resolution requires a large Hall coefficient (low carrier density) and low Johnson and 1/f noise. Low offset resistances are also a significant advantage in order to prevent the saturation of high gain, low noise preamplifiers. These criteria are all well satisfied in GaAs/AlGaAs heterostructure two-dimensional electron gases (2DEGs) at low temperatures, when they have very high carrier mobilities. Sensors with dimensions down to ~100 nm have been demonstrated and 2DEGs typically have low carrier concentration and are confined close to the surface of the chip [4]. However, the much lower carrier mobility at room temperature leads to much higher lead resistances and Johnson noise, and dramatically increases minimum detectable fields [5]. Moreover, low frequency 1/f noise increases rapidly at low Hall currents, further degrading minimum detectable fields. Other III-V semiconductor materials have been investigated with a view to achieving superior 300 K performance, including InSb thin films [6,7] ,as well as InAs/GaSb [8,9] and InGaAs/AlGaAs [10] quantum wells. Although somewhat improved figures of merit have been demonstrated in these alternative semiconductor systems at room temperature, all have associated limitations.

In practice semimetal Bi sensors prove to be superior to low carrier density semiconductor systems at 300 K, because much higher possible Hall probe currents and lower lead resistances outweigh the disadvantage of the considerably lower Hall coefficient. Thin Bi films do, however, suffer from the disadvantage that the carrier concentration depends quite strongly on a number of factors, e.g., substrate

material, deposition technique and film thickness. Scanning Bi Hall sensors have been widely investigated [11,12] and nanoscale devices with active sizes down to ~50 nm have been realised by focussed ion beam (FIB) milling of larger thin film structures [13-15]. However, it was found that devices smaller than 50 nm were not operational, presumably due to damage and Ga^+ ion incorporation during FIB milling [14]. These effects can be expected to increase device resistances and noise levels, and suggest that alternative fabrication methods could lead to improved figures of merit. Recently the use of lift-off techniques was demonstrated for fabricating low noise static nanoscale Bi Hall sensors for monitoring domain wall motion [16]. Here we extend this work to investigate the use of electron beam lithography and lift-off to fabricate scanning sub-micron Bi Hall sensors. We have systematically studied sensors as a function of Bi film thickness and active dimensions in the range 100 nm – 2 μm, and report the key figures of merit for our devices.

Experimental procedure

Sub-micron thin film Bi Hall effect sensors have been fabricated by optical and electron beam lithography and lift-off on semi-insulating GaAs substrates. Bismuth was selected for the active Hall element of our devices because, at room temperature, it has a low carrier density and relatively high carrier mobility. Two different Bi film thicknesses (50 nm and 70 nm) have been compared with the goal of optimising the sensor signal-to-noise ratio by exploiting the well-known dependence of the carrier density on thickness [17].

A semi-insulating GaAs wafer was diced into 6.5 mm x 6.5 mm square chips and four Hall sensors prepared on each chip, one in each quadrant. Cr(20 nm)/Au(200 nm) Ohmic contacts were first patterned by optical lithography, thermal evaporation and lift-off in acetone. Sub-micron Hall sensors, based on crosses defined by the intersection of two nanoscale wires, were then patterned in the poly methyl methacrylate (PMMA) by electron beam lithography, using the corners of the Cr/Au Ohmic contacts as alignment marks. Lumps of 99.999% purity Bi were etched in concentrated $HCl:H_2O$ (1:5) to strip surface oxides, and loaded into a Tungsten boat in a thermal evaporator. After pumping down, the samples were cleaned for 5 minutes in an Ar plasma and coated with 50 nm or 70 nm Bi films at a deposition rate of 0.25 – 0.5 nm/s, monitored with a quartz crystal thickness monitor. Hall probes based on wire widths in the range 0.1 - 2 μm were then realised by lift-off in hot

acetone in an ultrasonic bath. Contact resistances measured at this stage of fabrication were found to be unacceptably high (>750 kΩ). To rectify this a second Cr(10 nm)/Au(50 nm) metallisation was evaporated on top of the Bi leads, after which contact resistances were found to be very low (<10 Ω). Typically, two terminal resistances of completed sensors lie in the range 1-4 kΩ at room temperature. SEM images of a 0.1 μm wire width sensor fabricated in a 50 nm thick Bi film are shown in figure 1.

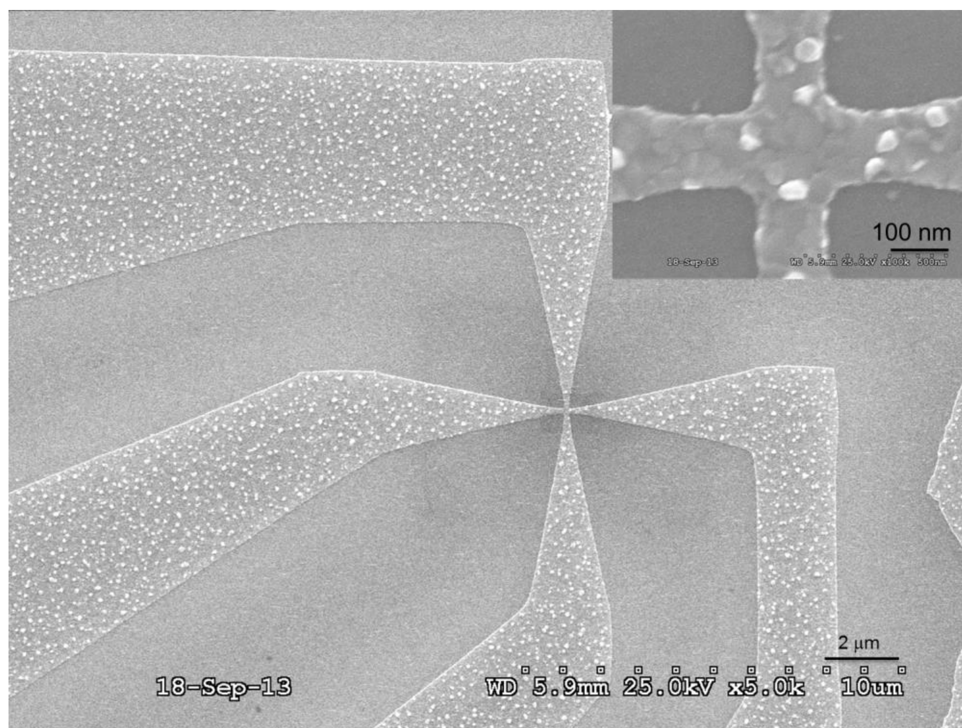

FIG. 1. SEM images at two different magnifications of a 50 nm thick Bi Hall probe based on the intersection of two 0.1 μm width wires.

The completed chips were glued with epoxy onto 0.5 mm thick 10 mm×10 mm alumina packages. These had been coated with gold leads which were wire bonded to the contacts on the chip with 25 μm Au wire. Long Cu wires were then Indium soldered to the leads on the package, for connection to terminals on the sample holder. The latter was the insert for a variable temperature cryostat and had 16 terminals on the sample plate connected by twisted pairs of Cu wires to BNC connectors in a connection box on top. The sample rod was inserted into the static sample space of a cryostat, evacuated and back-filled with Helium gas to prevent oxidation or other degradation of the Bi probes during characterisation. The tail of the cryostat containing the sample sits in the middle of a commercial electromagnet

capable of generating a maximum field of ~100 mT perpendicular to the plane of the sample. The electromagnet was driven by a bipolar power supply, allowing the magnetic field at the Hall sensor to be smoothly varied and reversed.

In order to characterise the Hall coefficient, sensors were driven with a 1-10 μA 32 Hz ac current from a commercial function generator in series with a 1 MΩ resistor. The Hall voltage and offset voltage were detected with a Stanford Research Systems SR830 digital lock-in amplifier. The sensor noise was characterised using a home-made battery-driven programmable dc current source and ultra-low noise preamplifier with 10^4 gain. Noise spectra were then measured in the range 0-100 Hz at fixed Hall currents with a Hewlett-Packard HP3561A dynamic signal analyzer. One hundred individual noise spectra were automatically averaged in the DSA to build the datasets presented below.

Experimental Results

Figure 2 shows the measured room temperature Hall coefficients for a large number of Hall probes with wire widths in the range 0.1 - 2 μm and a 10 μA Hall current. The graph shows data for sensors fabricated in both 50 nm (circles) and 70 nm (triangles) thick Bi Films. The data are consistent with the expectation that the Hall coefficient is constant for a given Bi thickness. However, we observe rather large fluctuations around the mean, that is indicated in each case by a horizontal dashed line, and is smaller for the 70nm probes (R_H(70 nm) ≅ 0.85 Ω/T) than the 50 nm probes(R_H(50 nm) ≅ 1.8 Ω/T). The large fluctuations from probe to probe are almost certainly linked to the rather random granularity of the Bi films, which can clearly be seen in the inset of Fig. 1. The grain structure in 70 nm films appears to be somewhat coarser than in the 50nm ones, explaining why we see the largest fluctuations in these sensors.

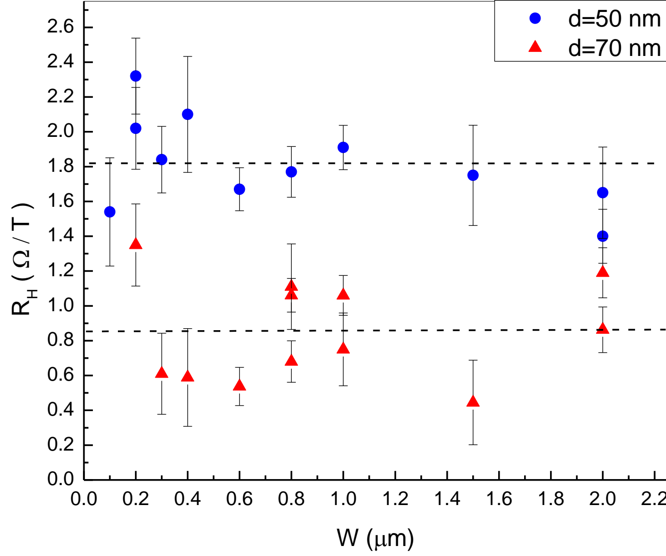

FIG. 2. (Color online) Measured room temperature Hall coefficient as a function of cross wire width for probes fabricated in 50 nm (circles) and 70 nm (triangles) thick Bi films.

In practice, the performance of Hall effect sensors can be limited by offset resistances arising from misalignment of Hall voltage contacts or spatially inhomogeneous current flow in the Hall probe itself. It is important to keep resulting offset voltages to a minimum, as they can limit the gain and fidelity of the preamplification stage used in the detection scheme. The offset resistance is defined as $R_{off} = V_H(H=0)/I_H$, where $V_H(H=0)$ is the Hall voltage at zero magnetic field and I_H is the Hall probe current. This is plotted in figure 3 for the same probes shown in Fig. 2. We find a very large spread in the distribution of offset resistances, with those for the 70 nm thick samples generally being larger than for the 50 nm samples. Again, we assume that this is related to the rather random granular structure of the films. In the smallest sensors the width of the active area is not much larger than the grain size, and inhomogeneous current flow through grains and grain boundaries is to be expected. However, for optimised structures the offset resistance can be as low as ~0.1 Ω, corresponding to an effective field of about 50-100 mT.

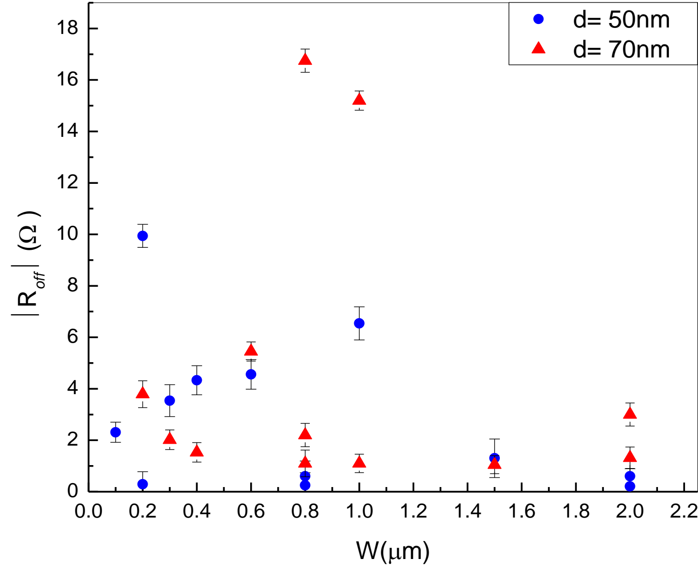

FIG. 3. (Colour online) Measured room temperature offset resistances as a function of cross wire width for probes fabricated in 50 nm (circles) and 70 nm (triangles) thick Bi films.

The signal-to-noise ratio (SNR) of our Hall sensors is limited by their frequency-dependent noise voltage, $V_n(f)$. At high frequencies, above the 1/f noise corner, this is governed by thermal Johnson noise, V_J [3]

$$V_J = \sqrt{4 R_V k_B T \Delta f}\,, \qquad (1)$$

where R_V is the resistance between the voltage leads, k_B is the Boltzmann constant, T is the temperature and Δf the measurement bandwidth. At low frequencies the spectrum is dominated by 1/f noise that has a wide range of possible origins, such as carrier fluctuations due to trapping/detrapping at defects or electron-hole generation-recombination processes [18]. The amplitude of the 1/f noise and the location of the 1/f noise corner increase quite rapidly as the sensor current increases.

Figure 4 shows typical noise spectra at three different Hall currents for a 0.3 μm wire width sensor fabricated in a 70 nm Bi film. These Data have been captured with a preamplifier gain of $G=10^4$. The horizontal dashed line indicates the high frequency Johnson noise floor, corresponding to a voltage lead pair resistance of 2.9 kΩ, close to the value of 3.5 kΩ measured independently. Clearly the low frequency noise

grows rapidly with Hall current and the 1/f shoulder simultaneously shifts to higher frequency, rising above our range of measurement frequencies at I_H=73 μA.

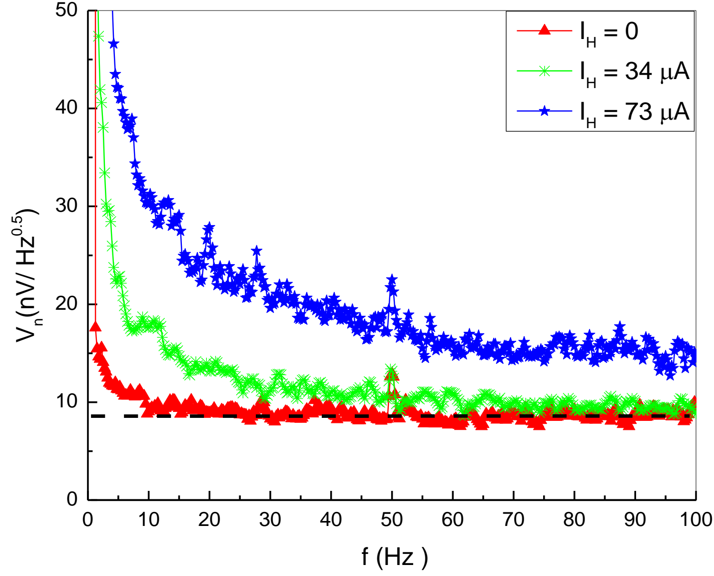

FIG. 4. (Colour online) Room temperature noise spectral density, V_n, as a function of measurement frequency for a 0.3 μm wire width Hall sensor patterned in a 70 nm Bi film at three Hall probe currents. The horizontal dashed line indicates the high frequency Johnson noise floor.

One of the most useful figures of merit for a Hall sensor is the minimum detectable field, B_{min}, defined by the magnetic field at which the Hall voltage equals the noise voltage. At frequencies above the 1/f noise corner this can be approximated by:

$$B_{\min} = \frac{\sqrt{4R_V k_B T \Delta f}}{I_H R_H}. \qquad (2)$$

This is plotted in Fig. 5 as a function of Hall cross wire width for various measurement currents. The minimum detectable field increases rapidly in smaller probes, due to their higher current densities for comparable Hall currents, and hence larger 1/f noise. We find that optimal Hall probes with wire widths ≥1 μm have minimum detectable fields ~0.1 mT/$Hz^{0.5}$ for Hall currents >70 μA, while deep sub-micron probes have values in the range (0.1-1) mT/$Hz^{0.5}$ for Hall currents in the range 5-20 μA.

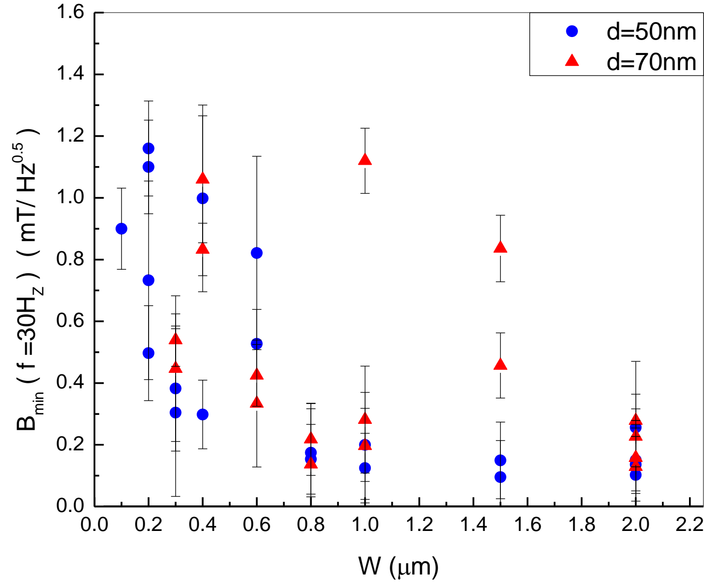

FIG. 5. (Color online) Room temperature minimum detectable fields (*f*=30 Hz) as a function of cross wire width for probes fabricated in 50 nm (circles) and 70 nm (triangles) thick Bi films.

Discussion

It is well established that the Hall coefficient of Bi thin films is a strong function of the substrate material, film thickness and deposition method/conditions [19]. The average Hall coefficients of 1.81 Ω/T(0.85 Ω/T) measured in sensors fabricated from 50 nm(70 nm) thick Bi films compares reasonably well with similar samples reported in the literature. Sandhu *et al.* [13] found R_H=4.0 Ω/T in a 50 nm probe milled by FIB in a 60 nm Bi film deposited on semi-insulating GaAs. This somewhat larger value could have arisen as a consequence of the much more rapid evaporation rate (~10 x faster) used to grow their Bi films, leading to a finer grain size and the loss of more free carriers to surface traps. Petit *et al.* [14] found R_H=1.73 Ω/T in a 750nm probe FIB milled in a 78 nm thick Bi film grown on an oxidised Si substrate. This is much closer to typical values measured in our sensors and any difference can probably be attributed to the different choice of substrate. Interestingly, Petit *et al.* also note a reduction of Hall coefficient with increasing current, and attribute this to an increase in the sensor temperature combined with a negative temperature coefficient for R_H(T). Very few publications report values for typical offset resistances. However, Petit *et al.* [15] state a value of 26.6 Ω in 40 nm wide probes FIB milled into a 50 nm thick Bi film. This is substantially larger than we typically measure in our smallest,

sensors, suggesting that FIB milling might significantly increase current inhomogeneity in such small devices.

We now compare the 300 K minimum detectable fields of our smallest sensors with similar sized devices reported in the literature. This is complicated by the fact that authors frequently present estimates based only on Johnson noise, corresponding to the limit when the measurement frequency is well above the 1/f noise corner. In general this significantly underestimates the true noise level. Adopting this approach initially, the high frequency minimum detectable fields for our 100nm sensors are ~10-80 $\mu T/Hz^{0.5}$ for Hall currents in the range 5-40 μA. This is reasonably consistent with 70 $\mu T/Hz^{0.5}$ in the 50 nm Bi probes of Sandhu *et al*. [13] and 5.1 $\mu T/Hz^{0.5}$ for the larger 750 nm Bi probes of Petit *et al*. [14]. Making a wider comparison with other materials systems we find reports of B_{min}~10 $\mu T/Hz^{0.5}$ for the 0.8 μm GaAs/AlGaAs sensors of Vervaeke *et al*. [5], 0.72 $\mu T/Hz^{0.5}$ for the 500nm InSb sensors of Gregory *et al.* [6] and Sandhu *et al*. [7], 0.5 $\mu T/Hz^{0.5}$ in the 5 μm GaSb/InSb probes of Grigorenko *et al*. [8] and Kazakova *et al*. [9] and 0.4 $\mu T/Hz^{0.5}$ in the 2 μm $In_{0.15}Ga_{0.85}As$ quantum well sensors of Pross *et al*. [10]. Since most of these devices are considerably larger than the smallest Bi probes measured here, the lower noise levels are not surprising. The noise figures for the 500 nm structures of Sandhu *et al*. [7] are impressive, but the growth of epitaxial InSb thin films remains a major challenge, and it is not clear that it would be possible to make these devices much smaller.

A more realistic estimate of minimum detectable fields is obtained by directly measuring the spectral noise density at typical operation frequencies. We have elected here to focus on the noise at 30 Hz, since this is the typical detection frequency used to operate our sensors, and assume that the noise spectrum with such a low frequency ac current approximates to that with a dc drive of the same mean density. For our 100 nm sensors fabricated from a 50 nm Bi film this yields an upper bound of B_{min}=0.9 $mT/Hz^{0.5}$ with a 5 μA Hall current. We note, however, that this current density was kept low to avoid risk of damage to the sensor and the optimal current density is probably up to ten times larger. Using larger currents in 200 nm and 300 nm sensors, the measured minimum detectable field dropped to 0.5 $mT/Hz^{0.5}$ and 0.3 $mT/Hz^{0.5}$ respectively. Petit *et al*. [14] report the measured noise spectra as a function of size for probes FIB milled from 78 nm Bi films. For a 100 nm

probe we interpolate a value of B_{min}(30Hz)~2 mT/$Hz^{0.5}$. This is significantly higher than in our somewhat thinner EBL sensors, possibly due to FIB induced damage and/or Ga^+ ion incorporation. However, we note that whenever we have equivalent sized Bi Hall probes to compare with, our best probes exhibit similar or better minimum detectable fields in all cases. Turning again to other materials systems, Vervaeke *et al.* [5] report optimum values of B_{min}(30Hz)~0.1mT/$Hz^{0.5}$ in 0.8 μm GaAs/AlGaAs sensors. At the same measurement frequency Kazakova *et al.* [9] report 0.056 mT/$Hz^{0.5}$ in 5 μm GaSb/InSb probes and Pross *et al.* [10] report 0.4 mT/$Hz^{0.5}$ in 2 μm $In_{0.15}Ga_{0.85}As$ quantum well devices.

Clearly the optimum minimum detectable fields for these alternative materials systems are all somewhat lower than we measure in our Bi sensors, but these data are for devices that are typically more than an order of magnitude larger than those we have studied here. Hence these semiconductor devices do not provide a comparable benchmark, and in some cases it is not even clear if their sizes could be reduced to deep sub-micron dimensions. Certainly the noise levels of our devices are lower than those reported for otherwise comparable FIB milled sensors. This suggests that the elimination of FIB damage and Ga^+ ion incorporation through the use of lift-off fabrication techniques does indeed lead to superior figures of merit in these Bi sensors.

There is still much that could be done to optimise the figures of merit of Bi Hall effect sensors. Recently Kubota *et al.* [16] have used advanced electron beam lithography and lift-off techniques to fabricate static 50 nm Hall probes in a 100 nm Bi film. The much thicker film yields lower lead resistances and allows much higher Hall currents to be used, and they report values of B_{min}~0.012 mT/$Hz^{0.5}$ measured at a frequency of 1000 Hz. The same approach could be used to optimise scanning sensors, although there is a price to pay in spatial resolution, since the local magnetic induction can no longer be assumed to be uniform throughout the depth of the film. A much more comprehensive study of the noise spectra, as a function of Hall current, is required to optimise sensor performance. In practice the increase in 1/f noise at higher drive currents is partially balanced by the higher effective sensitivity of the sensor, and a customised optimisation of each individual sensor is often required.

Finally, the microstructure of the films can still be improved to achieve better figures of merit. Sandhu *et al.* [13] find a much higher Hall coefficient in films which are

evaporated at very high deposition rates. High growth rates would also be expected to yield a finer-grained microstructure, leading to less current inhomogeneity and lower offset resistances. It has recently been demonstrated that nanoscale mechanical polishing of Bi films deposited on oxidised Si substrates leads to much smoother films, without degrading the crystal structure or resistivity [20]. This approach could be used to optimise the figures of merit of Hall devices, as well as enable the fabrication of even smaller sensors using advanced etching techniques.

Conclusions

In conclusion, we have demonstrated the fabrication of sub-micron Bi Hall effect sensors using electron beam lithography and lift-off techniques with active sizes in the range 0.1 - 2 μm. We have measured the key figures of merit of our sensors as a function of device dimensions for two different film thicknesses, and show that the minimum detectable fields of our smallest devices are superior to those fabricated by FIB milling of continuous Bi films. These sensors look very promising for applications in high resolution room temperature scanning Hall probe microscopy, and a number of ways in which their performance could be improved still further are discussed.

Acknowledgements

HAM acknowledges financial support for a PhD scholarship from the Ministry of Higher Education and Kirkuk University in Iraq. This work was supported by the Engineering and Physical Sciences Research Council (EPSRC) in the United Kingdom under grant nos. EP/J010626/1.

References

[1] Martin Y and Wickramasinghe H K 1987 Appl. Phys. Lett.. **50**, 1455

[2] Saenz J, Garcia N and Slonczewski J 1988 Appl. Phys. Lett., 1988 **53**, 1449

[3] Bending Simon J 1999 Adv. Phys. **48**, 449

[4] Hicks C *et al* 2007 Appl. Phys. Lett. **90**,133512

[5] Vervaeke K *et al* 2009 Rev. Sci. Inst, **80**, 074701

[6] Gregory A N, Bending S J and Sandhu 2002 Rev. Sci. Instrum. **73**, 3515

[7] Sandhu A *et al* 2004 Jpn. J. Appl. Phys. **43**, L868

[8] Grigorenko A N, Bending S J, Gregory J K and Humphreys R G 2001 Appl. Phys. Lett. **78**, 1586

[9] Kazakova O *et al* 2008 IEEE Trans. Magn **44**, 4480

[10] Pross A *et al 2005* J. Appl. Phys. **97**,096105

[11] Broom R F and Rhoderick E H 1962 Proc. Phys. Soc., **79**, 586

[12] Goren R N and Tinkham M 1971 J. Low Temp. Phys. **5**, 465

[13] Sandhu A *et al* 2004 Jpn. J. Appl. Phys. **43**, 777

[14] Petit D *et al 2004* IEE Proc.-Sci. Meas. Technol. **151**, 127

[15] Petit D *et al 2005* Rev. Sci. Insts. **76**, 026105

[16] Kubota M *et al* 2013 J. Appl. Phys. **114**, 0539009

[17] Boffoue M O *et al 2000* J. Phys. Chem. Solids **61**, 1979

[18] Hooge F 1994 IEEE Trans. Electr. Dev. **41**, 1926

[19] Hoffman R A and Frankl D R 1971 Phys. Rev. B **3**, 1825

[20] Koseva R *et al 2012* Thin Solid Films **520**, 5589